

188-20085023 Efficient Interior Noise Source Identification based on conformal mapping using SONAH holography for details on selected panels *

Jørgen HALD ¹⁾, Jakob MØRKHOLT ¹⁾, Jesper GOMES ¹⁾, Svend GADE ¹⁾

The present paper describes a set of array-based methods that can provide both a snapshot overview of problematic areas across the panels of a car cabin and perform efficient analysis of details of a noise problem. The snapshot overview is obtained with Beamforming, while detailed analysis of problematic areas is performed with a small planar single-layer or double-layer array in combination with SONAH holography. Using the SONAH algorithm for patch near-field acoustic holography, all sound field parameters can be estimated directly on the irregularly shaped panel surfaces. All the array measurements can be performed very efficiently by the use of a position measurement system integrated with the array. Panel geometry can also be measured using the position measurement system. The paper gives an overview of the different methods and presents results from a case study.

Key Words: NVH testing, Holography, Beamforming, Microphone array, Noise Source Identification

1. INTRODUCTION

Beamforming is an efficient tool for directional noise source location at medium-to-high frequencies, [1-2]. Basically the method provides an estimate of the contributions to the sound pressure at the array position from different directions. The resolution of the standard Delay-And-Sum Beamformer is limited to around one wavelength, which is very poor at the low frequencies. When applied in a cabin environment the method has the further limitation that it cannot distinguish directly radiated and reflected contributions. A spherical Beamformer in a perfectly diffuse field will just show that equal amounts of energy are incident from all directions. Car cabins are, however, sufficiently well damped that useful results can be obtained.

Near-field Acoustic Holography (NAH) can provide high resolution in the low-to-medium frequency range, and by mapping the sound intensity near the panels, the sound radiating areas will show up as opposed to purely reflecting areas: Total reflection at a panel surface will cause the reflected wave not to contribute to the normal component of the sound intensity on the surface. However, in order to deal with the fact that sound is incident from all sides, a double-layer array is in general needed in combination with a Patch Holography type of processing in order to distinguish waves coming from front and back. Traditional NAH requires the measurement area to fully cover the source in order to avoid severe spatial windowing effects. Patch NAH methods avoid the severe window effects, even when the measurement area is small compared to the source, [5].

Examples of Patch NAH methods are SONAH (Statistically Optimized NAH), [9-13], and HELS (Helmholtz equation least-squares), [6-8]. SONAH and HELS require basically planar and spherical source surface geometry, respectively, but good estimates of for example source surface vibration can be achieved even on irregular source surfaces, [13], [7]. A

comparison of SONAH and HELS was given in references [13], [19], including several simulated measurements. The present paper gives a short comparison.

The holography approach to be presented here is to measure small surface patches with a planar array and for each array position to backwards calculate the sound field parameters at the underlying source surface positions using SONAH. With integrated 3D position measurement in the array, a sequence of array positions can be quickly measured, providing both acoustic data and position data. If a CAD model of the source surface is not available, then the array position measurement system can be used to quickly measure a simple surface CAD model, which can then be meshed to get a grid of calculation positions. This procedure includes automatically an alignment between source geometry and measurement geometry. If on the other hand a CAD surface model is available, it can be directly imported and used.

Even with an efficient holography system it is a significant task to measure and map all interior surfaces of a cabin. If a beamforming system is used first to pinpoint suspected panel areas, then the holography measurement effort can be focused on these areas to get better resolution and to distinguish radiation from reflection.

2. SPHERICAL HARMONICS BEAMFORMING

Beamforming based on a spherical array has the advantage of being able to cover all directions and with direction independent angular resolution. We have used an array with the microphones flush-mounted on a rigid spherical surface, which has the advantage that cabling and integrated cameras can be hidden inside the sphere. A rigid surface also provides better numerical stability in connection with spherical harmonics beamforming than a transparent sphere, [2]. Figure 1 shows a 50-element array with 11 built-in cameras to cover all directions except a small angle around the floor stand.

The spherical harmonics beamforming with the 50-element spherical array of Figure 1 provides low sidelobe levels up to around 4 kHz. Above 4 kHz the sidelobe level slowly increases.

*Presented at 2008 JSAE Annual Congress, Yokohama, Japan.

1) Brüel & Kjær, Skodsborgvej 307, DK-2850 Nærum, Denmark.
E-mail: sgade@bksv.com, jhald@bksv.com, jmorkholt@bksv.com, jgomes@bksv.com

3. HIGH-RESOLUTION CONFORMAL MAPPING ON PANELS

As mentioned in the introduction, the Patch NAH method chosen here is SONAH. Another technique is HELS.



Fig. 1: Spherical array with 50 microphones and 11 small cameras flush mounted in a rigid spherical surface with diameter 19.5 cm

In brief, SONAH and HELS differ mainly in that SONAH uses a local plane wave expansion, while HELS uses a local spherical wave expansion. Due to the continuous nature of the plane wave spectrum, the SONAH calculations do not explicitly extract the plane wave coefficients. HELS computes the spherical wave coefficients. Beyond the regularization parameter, HELS involves the choice of two important parameters - the center of the spherical wave expansion and the number of waves to include - while SONAH needs only a single parameter - the distance to the virtual source plane. Measurement positions can be basically freely chosen in both methods, because of the least squares fit of model to data. No spatial FFT is performed. References [9-11].

4. HANDLING OF GEOMETRY

An important aspect of any practical conformal mapping system is the proper handling of the combined measurement and surface geometries. Basically, the positions of the sound pressure sampling points in space, relative to a set of surface sound field calculation points, must be known in order to set up the appropriate numerical sound field propagation model. This is illustrated in Figure 2a.

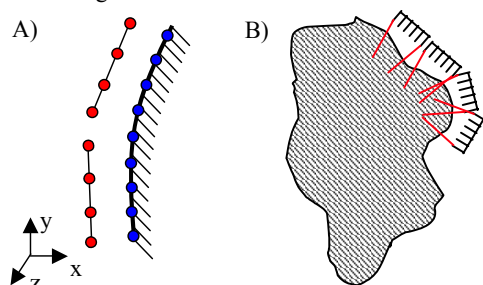


Fig. 2a: Sound field sampling point positions (red) relative to surface point positions (blue). Fig. 2b: Array patch measurements to cover a curved surface. Red lines mark the part of the surface corresponding to a given array position

The conformal mapping system used in the case study of this paper makes use of a small, planar microphone array mounted on a handle with a built-in 3D position measurement system, see Figure 3. The system continuously determines the

positions of the array microphones relative to some user-defined coordinate system. To map the sound field on a surface larger than the array, patch measurements are made with the array in neighboring (preferably overlapping) positions over the surface. See Figure 2b. In each array patch position, acoustic and position data belonging together is recorded. Patch positions already visited/measured are displayed in a 3D view along with the real-time updated current position of the array. Also shown in the 3D view is a surface model of the test object. In this way, the user is guided in covering the surface area with sufficient array patch positions in order to obtain a reliable surface mapping result. To minimize the errors in the patch holography calculations, a very small measurement distance is recommended, typically equal to half of the microphone grid spacing. If this is not possible, then patches with significant overlap should be used, avoiding the need to perform calculations near the boundaries of the array areas.

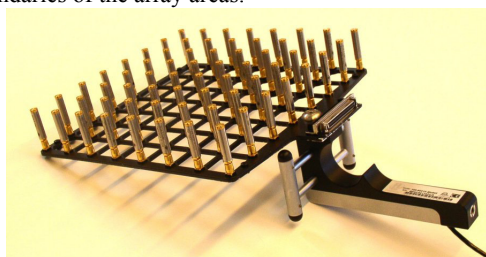


Fig. 3: Handheld array with 8x8=64 microphones and an InterSense IS900 position measurement system integrated in the handle. The microphones are Brüel & Kjær Type 4951 array microphones with TEDS that contain individual amplitude and phase responses of the microphones

The solution described in the case study of this paper attempts to combine the advantages of a “CAD-like” surface model with the advantages of being able to on-the-spot measure the rough geometry of the surface under investigation. To do this, the employed conformal mapping system includes functionality for synthesizing CAD-like surface models from point measurements on the surface. More specifically, various types of so-called Non-Uniform Rational Bézier-Spline or NURBS surfaces may be constructed from measured point data. NURBS curves and surfaces are parametric curve and surface descriptions widely recognized as the de facto industry standard for the representation, design and data exchange of geometric information processed by computers [16].

If on the other hand a suitable CAD surface model is available, the system allows for import of such a model via the IGES file format [17].

5. CASE STUDY

The present section illustrates the use of the described array measurement methods to localize noise problems in a car cabin. First, a controlled test was performed with two speakers outside the front right side-window of a Hyundai Sonata and, second, some results obtained with the conformal mapping system in GM’s wind tunnel near Detroit will be given.

The measurements were performed using a Brüel & Kjær PULSE system with a 65-channel Type 3560D front-end. The 50-element spherical array of Figure 1 was used for the beamforming measurements, and the 8x8 element single layer array of Figure 3 with 3 cm element spacing was used for the conformal mapping measurements. The array has a position measurement system built into its handle. Ideally a dual layer array should be used in a cabin environment with sound waves incident from both sides of the array, but unfortunately such an array was not available for the measurements. However, a cabin is typically well damped, and by measuring very near the panels, the direct field will in most cases dominate. Two of the array

microphones were used as references in all measurement with the handheld array. With the spherical array, the full cross spectral matrix was averaged and applied.



Fig. 4: Picture showing the spherical array on the front passenger seat and in the background the two speakers on the outside of the window

As shown in Figure 4, two small loudspeakers were mounted on the outside of the front right side window of a Hyundai Sonata car. Equal levels of incoherent pink noise excited the speakers. The spherical beamformer was set up approximately at the head position of a front-seat passenger to localize roughly, where the main contributions to the pressure at the head position enter the cabin. In this case the result is known: the area of the front right side window! But the plots will give an impression of the resolution provided by the spherical beamformer. Typically the maps will not have sufficient resolution to precisely identify the cause of a noise problem, and also reflections cannot be distinguished from direct radiation.

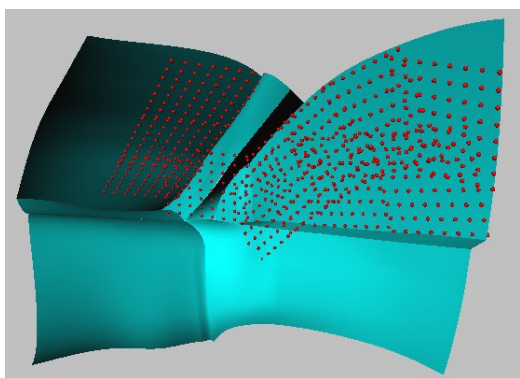


Fig. 5: On-the-spot digitized CAD geometry of the front right corner of the cabin with indication of measurement positions (red dots)

To obtain high resolution right on the curved panel surface, a conformal mapping was performed in the region of the front right side window. Figure 5 shows the panel geometry defined by the position measurement system, and the red dots represent the microphone positions covered by the applied set of array positions.

The results for the 1 kHz third octave band are shown in Figure 6a and 6b. The spherical beamformer (6a) clearly identifies the positions of the two speakers, but resolution is not sufficient to see if the noise is transmitted through the glass or if it is entering at the seals. The conformal map of normal sound intensity obtained from the patch measurements with the handheld array (6b) shows that the sound energy is entering mainly through the glass.

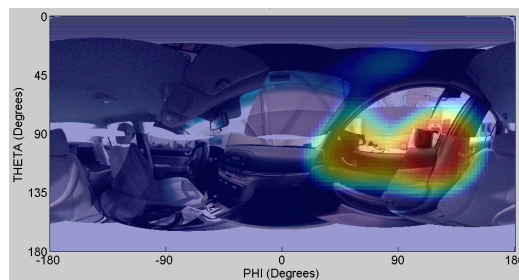


Fig. 6a: Beamformed map for the 1 kHz third octave band. Displayed dynamic range is 10 dB and threshold is 39 dB

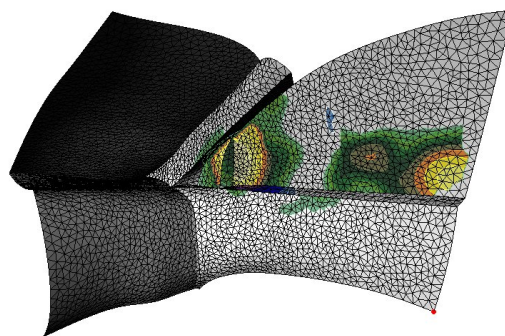


Fig. 6b: Conformal map of sound intensity for the 1 kHz third octave band. Displayed dynamic range is 15 dB and threshold is 58 dB

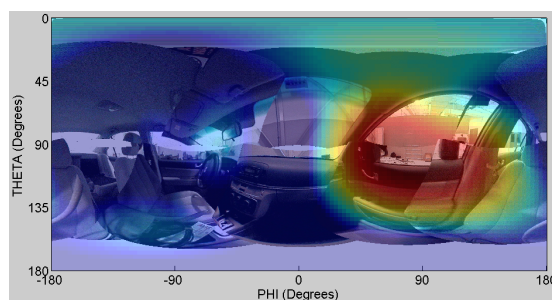


Fig. 7a: Beamformed map for the 630 Hz third octave band. Displayed dynamic range is 10 dB and threshold is 31.5 dB

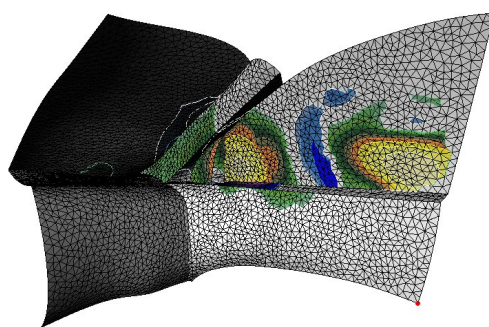


Fig. 7b: Conformal map of sound intensity for the 630 Hz third octave band. Displayed dynamic range is 15 dB and threshold is 59 dB

Figure 7a and 7b show the results for the 630 Hz third octave band. Here, the beamformed map (7a) cannot separate the two loudspeakers: There is a single broad peak at the bottom of the side-window, plus some lower level of reflection from the roof. The conformal sound intensity map (7b) shows clearly the two speakers and that the noise energy enters mainly through the glass.

6. WIND TUNNEL MEASUREMENTS

A test series were performed in the GM wind tunnel, with a set of measurements using the handheld array. The front left side window (near the driver's head position) was first digitized, providing the CAD model shown in figure 8.

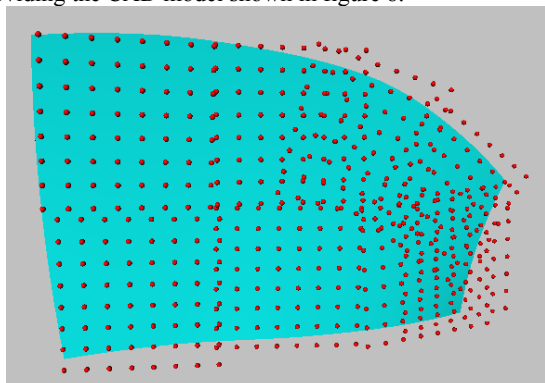


Fig. 8: Front left side window CAD model with measurement points (red dots)

Two measurements were performed in a mid size SUV at 0° yaw and 70mph wind speed: With (A) and without (B) the side mirror mounted. Figure 9 shows the corresponding calculated sound intensity maps at the side window for the 125Hz 1/3-octave band. Clearly, the presence of the mirror has a very significant effect covering the full length of the window. Corresponding sound intensity maps for the 200Hz and 315Hz 1/3-octave bands are shown in reference 18. At 200Hz the effect of the mirror still covers most of the length of the window, while at 315Hz the effect starts concentrating just behind the mirror, i.e. on the front window section. At the lowest frequencies a modal type of behavior is present.

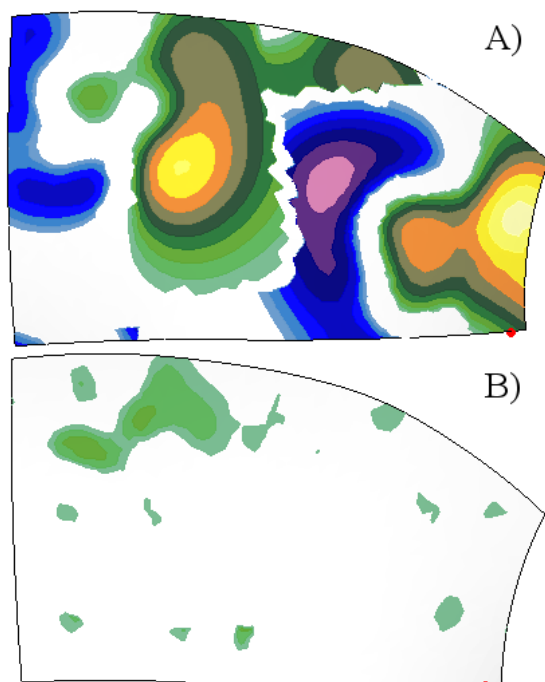


Fig. 9: Conformal maps of sound intensity for the 125 Hz third octave band: 9a) with mirror and 9b) without mirror. Displayed dynamic range is 10 dB and both plots have the same threshold

7. CONCLUSION

An array-based pair of tools has been presented, allowing very efficient, flexible and precise analysis of noise problems in cabin environments. First, panel sections with a possible high contribution to the noise level at a listening position are localized using a spherical array with built-in cameras. This is a one-shot measurement, but with limited spatial resolution, and without the capability of distinguishing radiated and reflected waves. To obtain higher resolution and to check whether hotspots represent radiation or reflection, a handheld array with a built-in 3D positions measurement system is applied to obtain a map of typically sound intensity directly on the suspected panel surface segments. If the panel geometry is available, it can be imported and aligned. If it is not, the 3D position measurement system can be applied to measure the panel surface geometry for the regions to be mapped.

REFERENCES

- (1) Christensen, J.J. and Hald, J., "Beamforming", *Brüel & Kjaer Technical Review*, No. 1, 2004.
- (2) Juhl, P.M., Petersen, S.O. and Hald, J., "Localizing sound sources in 3-D space using spherical harmonic beamforming", *Proceedings of Inter-noise 2005*.
- (3) Bowman, J.J., Senior, T.B.A. and Uslenghi, P.L.E., "Electromagnetic and acoustic scattering by simple shapes", Hemisphere Publishing Corporation, 1987.
- (4) Williams, E.G., "Fourier Acoustics", Academic Press, London, 1999.
- (5) Williams, E.G., "Continuation of acoustic near-fields," *Journal of the Acoustical Society of America*, 113(3), 1273-1281, 2003.
- (6) Wu, S.F., "On reconstruction of acoustic pressure fields using the helmholtz equation least squares method," *Journal of the Acoustical Society of America*, 107(5), 2511-2522, 2000.
- (7) Isakov, V. and Wu, S.F., "On theory and applications of the HELS method in inverse acoustics," *Inverse Problems*, 18, 1147-1159, 2002.
- (8) Wu, S.F. et al., "Diagnostics of Engine Noise During Run-up Using HELS Based Nearfield Acoustical Holography," *SAE Noise and Vibration Conference Proceedings*, 2005.
- (9) Steiner, R. and Hald, J., "Near-field Acoustical Holography without the errors and limitations caused by the use of spatial DFT," *International Journal of Acoustics and Vibration* 6(2), 83-89, 2001.
- (10) Hald, J., "Patch near-field acoustical holography using a new statistically optimal method," *Proceedings of Inter-Noise 2003*, 2203-2210, 2003.
- (11) Hald, J., "Patch holography in cabin environments using a two-layer handheld array with an extended SONAH algorithm," *Proceedings of Euronoise 2006*.
- (12) Gomes, J., "Comparing Parameter Choice Methods for the Regularization in the SONAH Algorithm," *Proceedings of Euronoise 2006*.
- (13) Hald, J. and Gomes, J., "A comparison of two patch NAH methods," *Proceedings of Inter-Noise 2006*.
- (14) Williams, E.G., "Approaches to Patch NAH," *Proceedings of Inter-noise 2003*, 2187-2194, 2003.
- (15) George, P.L. and Borouchaki, H., "Delaunay Triangulation and Meshing", Editions Hermes, Paris, 1998.
- (16) Piegl, L. and Tiller, W., "The NURBS Book", Monographs in Visual Communication, Springer, 1997.
- (17) "The Initial Graphics Exchange Specification (IGES) Version 5.x, Draft Baseline 1/99", IGES/PDES Organization, 1999.
- (18) Hald J., Mørkholt J., Gomes J., "Efficient Interior NSI based on various Beamforming methods for overview and conformal mapping using SONAH holography for details on selected panels", *SAE paper 07NVC-334*, 2007.
- (19) Gomes J., Jacobsen F., Bach-Andersen M., "Statistically optimised near field acoustic holography and the helmholtz equation least squares method: a comparison", *Proceedings of ICA*, 2007.